Mean zonal flow generated by azimuthal harmonic forcing in a rotating cylinder

A. Sauret

Surface du Verre et Interfaces, UMR 125, CNRS/Saint-Gobain, 93303 Aubervilliers, France

Department of Mechanical and Aerospace Engineering, Princeton University, Princeton, New Jersey 08544, USA

E-mail: `alban.sauret@saint-gobain.com`

Abstract. In this paper, we study analytically the flow in a rotating container subjected to an azimuthal forcing. We show that this mechanical forcing generates a correction to the solid body rotation called mean zonal flow, similarly to the time-oscillation of the rotation rate of an axisymmetric container. This axisymmetric correction induced by nonlinear effects in the Ekman layers modifies the solid-body rotation of the fluid in the container. At leading order, the contribution in the bulk is shown to be an azimuthal flow which scales as the square of the amplitude of the multipolar deformation and is independent of the Ekman number. We also show that the mean zonal flow depends on the symmetry of the angular forcing n and the ratio of the angular rate of the deformation and the angular rate of the cylinder $\Omega_R = \Omega_{orb}/\Omega_{spin}$. We found that for an elliptical forcing, $n = 2$ the rotation rate of the zonal flow does not depend on the radial position. In addition, the angular rate is found to be asymmetric with respect to Ω_R. These scalings are similar to the time harmonic forcing in a cylinder. The particular case of a tidal forcing is also considered.

Keywords: rotating flow, Ekman layers, mechanical forcing, mean zonal flow.

1. Introduction

Recent progress in astrophysical measurements have led to a renewed interest in the effects of a harmonic forcing on a rotating fluid. Indeed, harmonic forcings are ubiquitous in planetary bodies which are subject to various type of mechanical forcing due to the presence of other gravitational partners [19]. These harmonic forcings can be time dependent. For instance, a longitudinal libration forcing, corresponds to a time-harmonic oscillation of the rotation rate of a planet [7, 29]. For such a forcing, it has been shown that nonlinear effects in the Ekman layers generate a steady and axisymmetric flow, referred to as zonal flow. In a cylinder, an analytical description of this steady flow has been obtained by Wang [40] and successfully compared with experimental investigation. It has been shown that the deviation from a solid body rotation scales as the square of the amplitude of libration and is independent of the Ekman number. More recently, the limit of small libration frequency was considered [3] and the zonal flow in presence of inertial waves was studied numerically and experimentally [26, 22, 30]. However, this nonlinear correction is not limited to the cylindrical geometry and is also present in a sphere or spherical shell [1, 4, 33]. This geometry is particularly is relevant for geophysical and astrophysical applications [28]. Many recent studies have focused on this particular forcing as it is simple to implement in numerical simulations [30, 5, 31] and model with an experimental setup [28, 31]. In both geometries, it has been show that a centrifugal instability induced by the oscillation of the outer container could occur near the outer boundary [5, 30, 18]. However, we do not expect this kind of instability to occur in the system presented in this article.

However, other forcings are also present in astrophysical bodies, such as the precession forcing [2, 23] or the tidal forcing [38, 24, 19]. A planet or satellite is deformed into an elliptical shape by the presence of a gravitational partner. The gravitational field leads to an azimuthal forcing of azimuthal wavenumber $n = 2$. Recent experiments [25] and numerical simulation [39, 11] have considered a tidal forcing on a rotating sphere and showed that the resonance of inertial waves could lead to a strong zonal flow . In addition, this zonal flow can lead to a shear instability and turbulence [32]. An analytical study devoted to the mean zonal flow in a container elliptically deformed [38, 37] provided an analytical description of the nonlinear correction in a tidally deformed sphere and compared the results with some experiments. The study demonstrated that at first order, the base flow has elliptical streamlines [16]. However, the simple model of a sphere subject to a modulation of the tangential velocity with the azimuthal angle has several limitation. For instance, in this case, the fluid does not satisfy the continuity equation on the outer boundary. Finally, in a sphere, the forcing leads to a divergence of the zonal flow near the axis of rotation due to the presence of a critical latitude where the scalings of the Ekman layer no longer holds [17]. It remains unknown whether a multipolar deformation with an arbitrary azimuthal wavenumber leads to the same structure of the nonlinear correction. Moreover, the boundary conditions to apply on a deformed sphere are poorly defined as the deformed shape can lead to a variation in
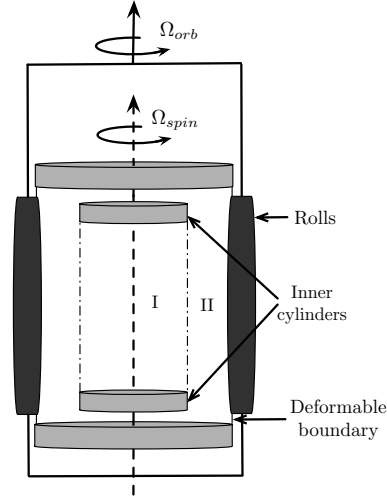
Figure 1. Experimental setup corresponding to the situation described in the article for $n = 2$. A flexible outer cylinder rotating at an angular velocity Ω_{spin} is deformed by two rolls rotating at a constant angular velocity Ω_{orb}. It generates elliptical streamlines in the bulk. Two cylindrical plates rotate at the velocity of the outer cylinder, Ω_{spin}. We are interested by the zonal flow generated in the region I.

the thickness of the Ekman layer.

In this paper, we aim to show that an azimuthal forcing exhibits the same key features as a temporal forcing. To carry a full analytical description without simplification on the shape of the outer boundary, we consider the simpler model of two cylindrical plates rotating in a multipolar flow where n is the symmetry of the angular forcing. The particular case $n = 2$ corresponds to an elliptical deformation. A schematic of the model geometry is presented in figure 1. Our analytical modeling demonstrates that the azimuthal forcing generates a steady axisymmetric differential rotation in the interior. This nonlinear effect scales as the mean zonal flow driven in a longitudinally librating cylinder. We also characterize the influence of the rotation of the deformation and the influence of the symmetry of the angular forcing, n, on the mean zonal flow generated.

2. Mathematical formulation

2.1. Multipolar deformation and generated flow

We consider the flow in an external cylindrical container of radius R_{ext} filled with an incompressible newtonian fluid of kinematic viscosity ν. The external container is deformable and rotates around its axis at a constant angular velocity Ω_{spin}. In addition a multipolar forcing rotating at the angular velocity Ω_{orb} is applied on the cylinder. The radius of the deformable boundary is given by

$$R_{ext}^{def}(\theta) = R_{ext} \left[1 + \frac{\beta}{n} \cos(n\,\theta) \right] + \mathrm{O}(\beta^2), \tag{1}$$
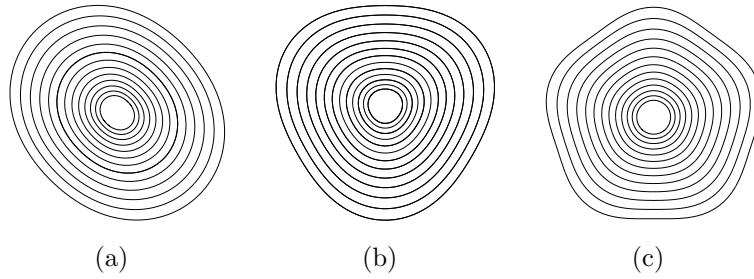
Figure 2. Streamlines induced by the multipolar deformation with $\beta = 0.1$ and r_{moy} ranging between 0.45 and 1 for (a) $n = 2$, (b) $n = 3$ and (c) $n = 5$.

where β and n are the amplitude and the symmetry of the angular forcing, respectively. To model an interaction between a satellite and its planet we generally consider only an elliptical deformation. However, the presence of other satellites can generate deformation with larger azimuthal wavenumber leading to a multipolar deformation. The resulting streamfunction can be written

$$\Psi = -\frac{r^2}{2} + \beta \frac{r^n}{n} \cos(n\theta) + \mathrm{O}(\beta^2), \tag{2}$$

with $n \geq 1$. The flow is the superposition of a solid body rotation and a multipolar strain field [21]. The shape of the streamlines is defined by $\Psi(r, \theta; \beta) = -k$ where k is a positive constant which is related to the mean radius by $r_{moy} = \sqrt{2\,k}$. The shape of a streamline is further characterized by a local deformation

$$\beta_n = \beta \left(\frac{2\,n\,k}{n-2}\right)^{(n-2)/2} \tag{3}$$

that measures its asymmetry. The streamlines for $\beta = 0.1$ and various the symmetry of the angular forcing n are represented in figure 2. Note that the case $\beta_n = \beta$ corresponds to a simple elliptical deformation, $n = 2$. In this case, the excentricity of the streamlines is constant and equal to $\beta_2 = \beta$. However, for $n \geq 3$, the deformation of the streamlines is no longer homogeneous when the constant k is modified. We notice that for small value of k, i.e. near the center of the flow, the streamlines are quasi-circular. Whereas for larger k values, further away from the center, the streamlines become more and more deformed and their local excentricity is defined by equation (3). Note also that for $\beta_n > 1$ the streamlines become open, thus the analysis will be restricted to the range $0 \leq \beta_n < 1$.

We define $\Omega_R = \Omega_{orb}/\Omega_{spin}$ as the ratio of the angular rate of the deformation and the angular rate of the cylinder. To simplify the situation, we consider two disks, separated by an axial distance H, and corotating with the cylinder around the (Oz)-axis at an angular rate equal to the angular rate of the external cylinder. A schematic of the situation is represented in figure 1. A similar system, without the inner disks, has been used by [9] to study the elliptical instability. Experimental measurements have shown that the generated elliptical streamlines are in good agreement with the equation

(2). Following the analytical study of the flow generated in an oscillating cylinder, we neglect the flow close to the corner. In the two regions indicated in Figure 1, (I) and (II), the flow has elliptical streamlines. We are interested in region (I) where no-slip boundary conditions have to be satisfied on the top and bottom cylinders which leads to the presence of viscous boundary layers, similarly to the situation of a libration-driven flow in a cylinder [40]. The nonlinear flow will be different in regions (I) and (II) leading to the presence of Stewartson layers between these two regions as observed previously in a spherical shell [33, 36]. However, for sake of simplification, we only consider the flow in region (I) and we do not consider the Stewartson layers that remains localized near the tangent cylinder between the two regions in the asymptotic analysis providing that the forcing is small enough. Indeed, we should emphasize that nonlinearities in the Stewarston layers could lead to instabilities that would broadened the Stewartson layers separating the region I and II and would modify the solution provided in this article [12, 14, 15, 34]. In addition, for instance for $n = 2$, an elliptical instability could develop at sufficiently large deformation [9, 16, 10, 19]. Therefore, our analysis applies for small enough forcing amplitude β for a given Ekman number E.

2.2. Dimensionless equations

We define the length scale and time scale of the problem as R_{ext}, the radius of the cylinder and Ω_{spin}^{-1}, respectively. In the following, we work in the rotating frame of angular velocity Ω_{orb}. In this frame of reference the flow is stationary and the non-dimensional Navier-Stokes and the continuity equations in cylindrical coordinates are given by:

$$u_r \frac{\partial u_r}{\partial r} + \frac{u_\theta}{r} \frac{\partial u_r}{\partial \theta} - \frac{u_\theta{}^2}{r} + u_z \frac{\partial u_r}{\partial z} - 2\,\Omega_R\,u_\theta \;\; = \;\; -\frac{\partial p}{\partial r} + E\,\nabla^2\,u_r \qquad (4a)$$

$$u_r \frac{\partial u_\theta}{\partial r} + \frac{u_\theta}{r} \frac{\partial u_\theta}{\partial \theta} + \frac{u_\theta\,u_r}{r} + u_z \frac{\partial u_\theta}{\partial z} + 2\,\Omega_R\,u_r \;\; = \;\; -\frac{1}{r}\frac{\partial p}{\partial \theta} + E\,\nabla^2\,u_\theta \qquad (4b)$$

$$u_r \frac{\partial u_z}{\partial r} + \frac{u_\theta}{r} \frac{\partial u_z}{\partial \theta} + u_z \frac{\partial u_z}{\partial z} \;\; = \;\; -\frac{\partial p}{\partial z} + E\,\nabla^2\,u_z \qquad (4c)$$

$$\frac{1}{r}\frac{\partial}{\partial r}(r\,u_r) + \frac{1}{r}\frac{\partial u_\theta}{\partial \theta} + \frac{\partial u_z}{\partial z} \;\; = \;\; 0 \qquad (4d)$$

where $E = \nu/(\Omega_{spin}\,H^2)$ is the Ekman number based on the height of the cylinder H. Considering a multipolar deformation [9, 20], the base flow in the bulk is given by

$$U_r \;\; = \;\; -\beta\,r^{n-1}\,(1 - \Omega_R)\,\sin(n\,\theta), \qquad (5a)$$

$$U_\theta \;\; = \;\; r\,(1 - \Omega_R) - \beta\,r^{n-1}\,(1 - \Omega_R)\,\cos(n\,\theta), \qquad (5b)$$

$$U_z \;\; = \;\; 0, \qquad (5c)$$

$$P \;\; = \;\; \frac{r^2}{2}\,(1 - \Omega_R{}^2) + \beta\,\frac{r^n}{n}\,[n\,(1 - \Omega_R) - 2]\,(1 - \Omega_R)\,\cos(n\,\theta). \qquad (5d)$$

For a fixed deformation $\Omega_R = 0$ and an elliptical forcing $n = 2$, we recover the base flow of a tidal deformation [16]. Note that in the following we will use the notation (U_r, U_θ, U_z, P) for the velocity and pressure fields in the bulk and (u_r, u_θ, u_z, p) for the velocity and pressure fields in the Ekman layers.

3. Linear solution in the top and bottom boundary layers

The velocity and pressure fields (5a)-(5d) are solutions of the Navier-Stokes and continuity equations. However, the velocity is not constant along a streamline, it is lower in the region with a larger curvature. In addition, at the bottom and top boundaries ($z = [0; H]$), the flow has to satisfy no-slip boundary conditions. On these boundaries, in the rotating frame with the deformation the no-slip conditions are a solid body rotation at an angular velocity $\Omega_{spin} - \Omega_{orb}$. To satisfy these boundary conditions, we need to introduce a viscous layer to match the flow in the bulk with the condition on the solid boundary. For instance, we consider the viscous layer near the bottom boundary, at $z = 0$. Note that, the system is symmetric, we therefore expect the same flow to happen at the top boundary. Let us introduce the boundary layer coordinate:

$$\zeta = \frac{z}{E^{1/2}} \tag{6}$$

To perform the asymptotic analysis, we assume that the velocity field and the pressure can be expanded in a power series of β and $E^{1/2}$:

$$\mathbf{u} = \mathbf{u}_0 + \sum_{i=1,j=0} E^{j/2}\,\beta^i\,\mathbf{u}_i^j, \tag{7}$$

$$p = p_0 + \sum_{i=1,j=0} E^{j/2}\,\beta^i\,p_i^j. \tag{8}$$

In the following, to simplify the notation, we only indicate the order in β. Assuming that the radial and orthoradial components of the velocity fields, u_r and u_θ, are of order E^0 in the boundary layer, equation (4.d) indicates that the axial velocity is of order $E^{1/2}$ smaller in the boundary layer. Thus, in the boundary layers equations (4a)-(4c) can be reduced to the leading order in E and at the order β:

$$\frac{u_{0,\theta}}{r}\frac{\partial u_{1,r}}{\partial \theta} - \frac{2\,u_{0,\theta}\,u_{1,\theta}}{r} - 2\,\Omega_R\,u_{1,\theta} = -\frac{\partial p_1}{\partial r} + \frac{\partial^2 u_{1,r}}{\partial \zeta^2} \tag{9a}$$

$$u_{1,r}\frac{\partial u_{0,\theta}}{\partial r} + \frac{u_{0,\theta}}{r}\frac{\partial u_{1,\theta}}{\partial \theta} + \frac{u_{0,\theta}\,u_{1,r}}{r} + 2\,\Omega_R\,u_{1,r} = -\frac{1}{r}\frac{\partial p_1}{\partial \theta} + \frac{\partial^2 u_{1,\theta}}{\partial \zeta^2} \tag{9b}$$

$$\frac{\partial p_1}{\partial \zeta} = 0 \tag{9c}$$

where $u_{0,\theta}$ is the solution of order 0 in β. The equation (9c) leads to a constant pressure field in the boundary layer. Its expression is therefore directly given by equation (5d). The symmetry of the multipolar forcing associated to a symmetry of the angular forcing n, sets the symmetry of the velocity field

$$u_{1,r} = \beta\,\tilde{u}_{1,r}\,\mathrm{e}^{\mathrm{i}n\theta} + \text{c.c} \quad \text{and} \quad u_{1,\theta} = \beta\,\tilde{u}_{1,\theta}\,\mathrm{e}^{\mathrm{i}n\theta} + \text{c.c.} \tag{10}$$

From the equations (9a)-(9b) and with the leading order solution, we obtain the following equations:

$$i\,n\,(1 - \Omega_R)\,\tilde{u}_{1,r} - 2\,\tilde{u}_{1,\theta} = -\frac{\partial \tilde{p}_1}{\partial r} + \frac{\partial^2 \tilde{u}_{1,r}}{\partial \zeta^2} \tag{11a}$$

$$2\,\tilde{u}_{1,r} + i\,n\,(1 - \Omega_R)\,\tilde{u}_{1,\theta} = -\frac{i\,n\,\tilde{p}_1}{r} + \frac{\partial^2 \tilde{u}_{1,\theta}}{\partial \zeta^2} \tag{11b}$$

For $\zeta = 0$, i.e. at the boundary of the cylinder, the velocity field vanishes at first order in β. Therefore, we impose the following boundary conditions:

$$\tilde{u}_{1,r}(\zeta = 0) = 0, \quad \tilde{u}_{1,\theta}(\zeta = 0) = 0, \quad \tilde{u}_{1,\zeta}(\zeta = 0) = 0. \tag{12}$$

We note that the velocity field at order 0, $\tilde{u}_0$, needs to fulfill the no-slip boundary conditions at the upper and lower boundaries. Then, the matching condition between the flow in the boundary layer and the flow in the bulk leads to

$$\lim_{\zeta \to +\infty} \tilde{u}_{1,r} = -\frac{r^{n-1}\,(1 - \Omega_R)}{2\,i}, \quad \lim_{\zeta \to +\infty} \tilde{u}_{1,\theta} = -\frac{r^{n-1}\,(1 - \Omega_R)}{2}, \quad \text{and } \lim_{\zeta \to +\infty} \tilde{u}_{1,\zeta} = 0. \tag{13}$$

Finally, the solution this array of equations is given by:

$$\tilde{u}_{1,r} = i\,\frac{r^{n-1}\,(1 - \Omega_R)}{2}\,(1 - e^{-\lambda \zeta}) \tag{14a}$$

$$\tilde{u}_{1,\theta} = -\frac{r^{n-1}\,(1 - \Omega_R)}{2}\,(1 - e^{-\lambda \zeta}) \tag{14b}$$

$$\tilde{u}_{1,z} = 0 \tag{14c}$$

$$\tilde{p}_1 = = \frac{r^n}{2\,n}\,[n\,(1 - \Omega_R) - 2]\,(1 - \Omega_R) \tag{14d}$$

where δ is the boundary layer thickness,

$$\lambda = (1 + s_\pm\,i)\left|\frac{n}{2}\,(1 - \Omega_R) - 1\right|^{1/2} \tag{15}$$

with

$$s_\pm = 1 \quad \text{if} \quad \frac{n}{2}\,(1 - \Omega_R) - 1 > 0,$$

$$s_\pm = -1 \quad \text{if} \quad \frac{n}{2}\,(1 - \Omega_R) - 1 < 0.$$

From expressions (14a)-(14d), we obtain the velocity field and the pressure in the boundary layer:

$$u_{1,r} = -r^{n-1}\,(1 - \Omega_R)\left[\sin(n\,\theta) - \exp(-\delta\,\zeta)\,\sin(n\,\theta + s_\pm\,\delta\,\zeta)\right] \tag{16a}$$

$$u_{1,\theta} = -r^{n-1}\,(1 - \Omega_R)\left[\cos(n\,\theta) - \exp(-\delta\,\zeta)\,\cos(n\,\theta + s_\pm\,\delta\,\zeta)\right] \tag{16b}$$

$$u_{1,z} = 0 \tag{16c}$$

$$p_1 = = \frac{r^n}{n}\,[n\,(1 - \Omega_R) - 2]\,(1 - \Omega_R)\,\cos(n\,\theta) \tag{16d}$$

where we have defined

$$\delta = \left|\frac{n}{2}\,(1 - \Omega_R) - 1\right|^{1/2} \tag{17}$$

4. Non-linear correction

In the previous section, we have showed that the linear response of the flow to a multipolar deformation is a correction at order β with harmonics $e^{in\theta}$ and $e^{-in\theta}$. The nonlinear contribution, i.e. β^2 terms, comes from the nonlinear interactions of the linear flow with itself in the top and bottom Ekman layers and generates harmonics $e^{2in\theta}$, $e^{-2in\theta}$ and $e^{i0} = 1$. This last term is referred to as the zonal flow. It represents a drift of the fluid during the rotation of the fluid and contributes to the flow after one rotation.

4.1. Non linear flow in the bulk

Contrary to the longitudinal libration forcing where the linear correction is of order $\varepsilon\sqrt{E}$ in the bulk [40, 3, 33], here we have to consider the linear correction of order βE^0 in the bulk and study if its nonlinear interaction leads to a mean zonal flow, i.e. to a contribution of harmonics e^{i0}. In the bulk at order β^2, the Navier-Stokes equation leads to

$$r^{2n-3}(n-1)(1-\Omega_R{}^2) - 2U_{2,\theta} = -\frac{\partial P_2}{\partial r}, \tag{18a}$$

$$U_{2,r} = 0 \tag{18b}$$

$$U_{2,z} = 0 \tag{18c}$$

Indeed, the nonlinear contribution through the term $\mathbf{U} \cdot \nabla\mathbf{U}$ vanishes, and does not generate a nonlinear axisymmetric flow in absence of top and bottom viscous layers. The physical effects that generate a mean zonal flow in the bulk are thus the same as for a temporal forcing. Actually, the equations (18a)-(18c) mean that the nonlinear and axisymmetric component of the velocity field only depends on the cylindrical radial coordinate r and can be written:

$$U_{2,\theta} = r\,\Omega_2(r) \tag{19}$$

where Ω_2 is only a function of r to be determined. The aim of the next section is to obtain an expression for this function.

4.2. Non linear axisymmetric solution in the boundary layers

At the order β^2, equations (4a)-(4c) in the boundary layer at the order β^2 simplify to:

$$u_{1,r}\frac{\partial u_{1,r}}{\partial r} + \frac{u_{1,\theta}}{r}\frac{\partial u_{1,r}}{\partial \theta} - \frac{u_{1,\theta}{}^2}{r} - 2\,u_{2,\theta} = -\frac{\partial p_2}{\partial r} + \frac{\partial^2 u_{2,r}}{\partial \zeta^2} \tag{20a}$$

$$u_{1,r}\frac{\partial u_{1,\theta}}{\partial r} + \frac{u_{1,\theta}}{r}\frac{\partial u_{1,\theta}}{\partial \theta} + \frac{u_{1,\theta}\,u_{1,r}}{r} + 2\,u_{2,r} = \frac{\partial^2 u_{2,\theta}}{\partial \zeta^2} \tag{20b}$$

$$\frac{\partial p}{\partial \zeta} = 0 \tag{20c}$$

Substituting the expressions (11a-d), we obtain

$$\frac{\partial^2 u_{2,r}}{\partial \zeta^2} + 2\, u_{2,\theta} = \frac{\partial p_2}{\partial r} + r^{2\,n-3}\,(n-1)\,(1-\Omega_R)^2\,(1-e^{-\lambda\zeta})\,(1-e^{-\lambda^*\zeta})$$

$$(21a)$$

$$\frac{\partial^2 u_{2,\theta}}{\partial \zeta^2} - 2\, u_{2,r} = 0 \qquad\qquad (21b)$$

This leads to a differential equation in ζ for $(u_{2,r} + i\,u_{2,\theta})$:

$$\left(\frac{\partial^3}{\partial \zeta^3} - 2\,i\,\frac{\partial}{\partial \zeta}\right)(u_{2,r} + i\,u_{2,\theta}) = r^{2\,n-3}\,(n-1)\,(1-\Omega_R)^2\left(\lambda\,e^{-\lambda\zeta}\right.$$

$$\left. + \lambda^*\,e^{-\lambda^*\zeta} - (\lambda+\lambda^*)e^{-(\lambda+\lambda^*)\zeta}\right) \quad (22)$$

We write the no-slip conditions on the bottom boundary, i.e. for $\zeta = 0$,

$$u_{2,r}(\zeta = 0) = 0 \qquad \text{and} \qquad u_{2,\theta}(\zeta = 0) = 0 \qquad\qquad (23)$$

Morevoer, the matching condition between the solution in the Ekman layer and the solution in the bulk leads to

$$\lim_{\zeta\to+\infty} u_{2,r} = 0 \qquad \text{and} \qquad \lim_{\zeta\to+\infty} u_{2,\theta} = i\,r\,\Omega_2(r) \qquad (24)$$

Therefore, the solution to equations (22)-(24) is

$$u_{2,r} + i\,u_{2,\theta} = r^{2\,n-3}\,(n-1)\,(1-\Omega_R)^2\left[\frac{e^{-\kappa\zeta} - e^{-(\lambda+\lambda^*)\zeta}}{\kappa^2 - (\lambda+\lambda^*)^2} - \frac{e^{-\kappa\zeta} - e^{-\lambda\zeta}}{\kappa^2 - \lambda^2}\right.$$

$$\left. - \frac{e^{-\kappa\zeta} - e^{-\lambda^*\zeta}}{\kappa^2 - \lambda^{*2}}\right] + i\,r\,\Omega_2(r)\,(1 - e^{-\kappa\zeta}) \qquad (25)$$

where $\kappa = 1 + i$. The continuity equation in the boundary layer for the nonlinear and axisymmetric flow, $\beta^2\,e^{i\,0}$, writes

$$\frac{\partial}{\partial r}(r\,u_{2,r}) + \frac{1}{\sqrt{E}}\frac{\partial u_{2,z}}{\partial \zeta} = 0 \qquad\qquad (26)$$

As $U_{2,r} = 0$ and $U_{2,\theta}$ is only function of r, the continuity equation in the bulk implies that the axial velocity does not depend on the axial coordinate z:

$$\frac{\partial U_{2,z}}{\partial z} = 0 \qquad\qquad (27)$$

Moreover, the system exhibits an equatorial symmetry. Therefore, we have for $z = H/2$, $U_{z,2} = 0$. As a consequence, in all the bulk, $U_{2,z} = 0$. Thus, to satisfy the matching condition in the bulk, the equation (26) implies that $u_{2,r}$ satisfies the relation:

$$\lim_{\zeta\to+\infty} u_{2,z} = -\sqrt{E}\int_0^{+\infty}\frac{\partial}{\partial r}(r\,u_{2,r})\,\mathrm{d}\eta = 0 \qquad (28)$$

Let us inject the solution (25) in the relation (28). We then obtain a differential equation for $\Omega_2(r)$ with $S > 0$:

$$\frac{r^2}{2}\frac{\mathrm{d}\Omega_2(r)}{\mathrm{d}r} + r\,\Omega_2(r)$$

$$+ \frac{r^{2\,n-3}\,(n-1)^2\,(1-\Omega_R)^2\,[1 - S\,[2 + S\,(10\sqrt{S} - 2\,S - 9)]]}{2\,(4\,S^2 + 1)\,(S^2 - 1)} = 0 \qquad (29)$$

where S is defined by

$$S = \left| \frac{n}{2} (1 - \Omega_R) - 1 \right| \tag{30}$$

The constant of integration has to be taken equal to zero to avoid the divergence of $\Omega_2(r)$ at $r = 0$. Finally, the solution is given by

$$\Omega_2 = -\frac{r^{2n-4} (n-1)^2 (1 - \Omega_R)^2 [1 - S[2 + S(10\sqrt{S} - 2S - 9))]]}{2 (4S^2 + 1)(S^2 - 1)} \tag{31}$$

5. Discussion

From expression (31), we see an important difference between an elliptical forcing, $n = 2$ and an higher order azimuthal forcing, $n > 2$. For $n = 2$, the structure of the rotation rate associated with the mean zonal flow is the same as for a longitudinal libration forcing [40]: the rotation rate does not depend on the radius. Whereas for larger values of n, Ω_2 depends on the radial position in the flow. We have plotted the angular rotation rate Ω_2, associated with the zonal flow for $n = 2$ in figure 3. The mean zonal flow vanishes for $\Omega_R = 1$, i.e., at an angular rate of the deformation equal to the angular rate of the cylinder. Here, the flow is only a solid body rotation in the bulk and no pumping is generated in the top and bottom Ekman layers. Note also a singular point for $\Omega_R = 1 - 2/n$, for example $\Omega_R = 0$ for an elliptical deformation, $n = 2$. In this situation, $S = 0$ and the Ekman layer becomes singular: the calculation presented in this article cannot be used anymore. However, we note that the plot shown in figure 3 can be smoothed by continuity around this critical value as observed in an oscillating cylinder [40]. The correction can also be cyclonic or anticyclonic as it is positive for

$$\frac{n-2}{n} - \frac{2[1 + 2^{1/3} + 2^{2/3}]}{n} < \Omega_R < \frac{n-2}{n} + \frac{2[1 + 2^{1/3} + 2^{2/3}]}{n} \tag{32}$$

and decreases to $-\infty$ for large value of Ω_R.

Figure 4 shows the mean rotation rate Ω_2 for a given value of $\Omega_R = 2$ and various values of the azimuthal wavenumber of the perturbation. As mentioned previously, the elliptical forcing is the only case where the angular velocity associated to the mean zonal flow does not depend on the radius. Increasing the azimuthal wavenumber of the forcing leads to a flattening of the angular rate near the axis of rotation and an increase of the value at $r = 1$. This result is in agreement with the definition of the local curvature (3) given in the introduction of the article.

We should also mention that owing to the deviation from the solid-body rotation between the two cylindrical plates, the axisymmetric flow in the interior (for $r < 1$) does not rotate at the same velocity as in the outer region ($r > 1$). Therefore, this discontinuity will be smooth in Stewartson layer exhibiting the same structure as in two cylindrical plates rotating at different velocities [35, 36]. The presence of such layers was already described for a time-harmonic forcing in a rotating shell [33] where it was in rather good agreement with numerical simulations.
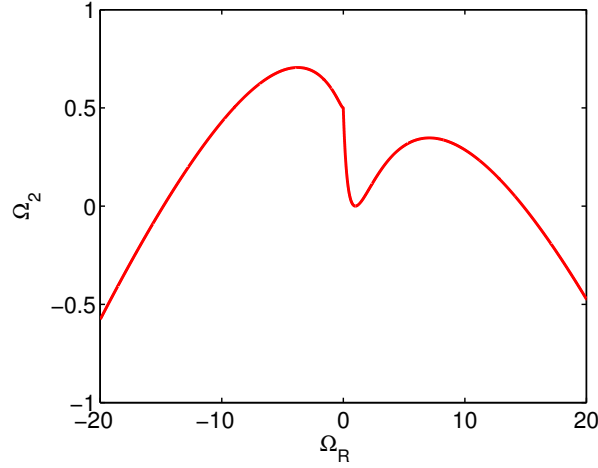
Figure 3. Angular rate associated to the mean zonal flow generated by an elliptical forcing, $n = 2$ in the cylinder (red continuous line).
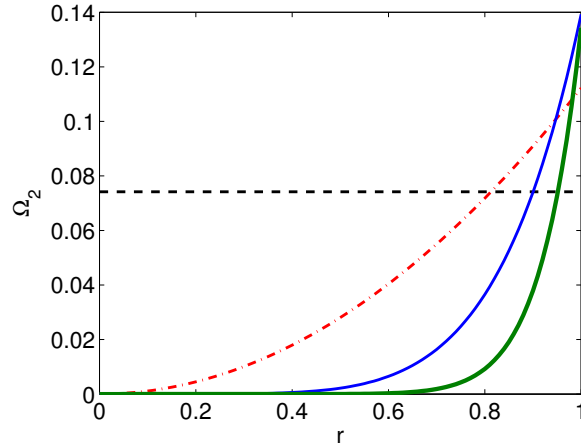

Figure 4. Angular rate associated to the mean zonal flow generated by various multipolar forcing in the cylinder for $\Omega_R = 2$. The dashed black line is an elliptical forcing, $n = 2$; red dashed-dotted line is a tripolar forcing, $n = 3$; blue continuous line corresponds to $n = 5$ and the green thick continuous line is $n = 8$.

We have considered the flow in the inner region (I), but we should notice that in the region (II) (see figure 1), the elliptical streamlines also induced a correction near the external boundary at $r = R_{ext}$. In the limit of the small deformations, $\beta \ll 1$, the correction at first order in β writes [8]:

$$U_r = -\beta\, r^{n-1}\, (1 - \Omega_R)\, \sin(n\,\theta) - (1 - \Omega_R)\, \frac{\beta\, \sqrt{E}\,(1 - n)}{\sqrt{n}}\, \mathrm{e}^{k_\nu\,(r - R_{ext})}$$

$$\times \sin\left(k_\nu\,(r - R_{ext}) + n\,\theta + \frac{\pi}{4}\right),(33)$$

$$U_\theta = r\,(1 - \Omega_R) - \beta\, r^{n-1}\,(1 - \Omega_R)\, \cos(n\,\theta) - (1 - \Omega_R)\, \frac{\beta\, k_\nu\, \sqrt{E}\,(1 - n)}{n^{3/2}}\, \mathrm{e}^{k_\nu\,(r - R_{ext})}$$

$$\times \left[\cos\left(k_\nu \left(r - R_{ext} \right) + n\,\theta + \frac{\pi}{4} \right) - \sin\left(k_\nu \left(r - R_{ext} \right) + n\,\theta + \frac{\pi}{4} \right) \right], \quad (34)$$

$$U_z = 0, \tag{35}$$

where we defined

$$k_n = \sqrt{\frac{n}{2\,E}}. \tag{36}$$

In this paper, we have demonstrated the similarity of the mean zonal flows generated by a time harmonic and an azimuthal forcing between two cylindrical plates. However, in addition to the mean zonal flow, inertial waves are also susceptible to appear depending on the frequency of perturbation. In a cylinder driven by longitudinal libration at the frequency ω of its outer boundary, the emitted inertial waves satisfy the dispersion relation $\omega = 2\sin\theta$ where θ is the angle between the direction of propagation of the inertial waves and the axis of rotation [13, 42]. For a multipolar forcing, we expect to see the propagation of inertial waves in the range

$$n - 2 < \omega < n + 2 \tag{37}$$

To conclude, we have demonstrated the analogy between time and azimuthal forcings in a rotating cylinder. We note that the same analogy is expected to be present in a rotating sphere or shell. However, in this geometry, the boundary conditions are more complicated to apply and the presence of a critical latitude may lead to a divergence of the flow at some particular point [4, 17]. In addition, the longitudinal libration of an ellipsoid is of importance for geophysical and astrophysical applications and will also needed to be considered [27, 41, 6]. This paper therefore constitutes a first step toward understanding the effect of both time harmonic and azimuthal forcings on the mean zonal flow in ellipsoidal containers and astrophysical bodies.

Acknowledgments

References

[1] K. D. Aldridge. *An experimental study of axisymmetric inertial oscillations of a rotating liquid sphere.* PhD thesis, Massachusetts Institute of Technology, 1967.

[2] F. H. Busse. Steady fluid flow in a precessing spheroidal shell. *J. Fluid Mech.*, 33:739–751, 1968.

[3] F. H. Busse. Zonal flow induced by longitudinal librations of a rotating cylindrical cavity. *Physica D: Nonlinear Phenomena*, 240:208–211, 2011.

[4] F.H. Busse. Mean zonal flows generated by librations of a rotating spherical cavity. *J. Fluid Mech.*, 650:505–512, 2010.

[5] M. A. Calkins, J. Noir, J. Eldredge, and J. M. Aurnou. Axisymmetric simulations of libration-driven fluid dynamics in a spherical shell geometry. *Physics of Fluids*, 22:1–12, 2010.

[6] K. H. Chan, X. Liao, and K. K. Zhang. Simulations of fluid motion in ellipsoidal planetary cores driven by longitudinal libration. *Physics of the Earth and Planetary Interiors*, 187:391–403, 2011.

[7] R. L. Comstock and B. G. Bills. A solar system survey of forced librations in longitude. *Journal of Geophysal Research*, 108:113, 2003.

[8] C. Eloy. *Instablité multipolaire de tourbillons*. PhD thesis, Université Aix-Marseille II, Institut de Recherche sur les Phnomnes Hors Equilibre, 2000.

[9] C. Eloy, P. Le Gal, and S. Le Dizès. Experimental study of the multipolar vortex instability. *Phys. Rev. Lett.*, 85:3400–3403, 2000.

[10] C. Eloy, P. Le Gal, and S. Le Dizès. Elliptic and triangular instabilities in rotating cylinders. *J. Fluid Mech.*, 476:357–388, 2003.

[11] B. Favier, A. J. Barker, C. Baruteau, and G. I. Ogilvie. Non-linear evolution of tidally forced inertial waves in rotating fluid bodies. *Mon. Not. Roy. Astron. Soc.*, 439:845–860, 2014.

[12] W. G. Fruh and P. L. Read. Experiments on a barotropic rotating shear layer. part 1. instability and steady vortices. *J. Fluid Mech.*, 383:143–173, 1999.

[13] H. P. Greenspan. *The Theory of rotating fluids*. Cambridge University Press, Cambridge, 1968.

[14] R. Hollerbach. Instabilities of the stewartson layer part 1. the dependence on the sign of *ro*. *J. Fluid Mech.*, 492:289–302, 2003.

[15] R. Hollerbach, B. Futterer, T. More, and C. Egbers. Instabilities of the stewartson layer part 2. supercritical mode transitions. *Theor. Comp. Fluid Dyn.*, 18:197–204, 2004.

[16] R. R. Kerswell. Elliptical instability. *Annual Review of Fluid Mechanics*, 34:83–113, 2002.

[17] S. Kida. Steady flow in a rapidly rotating sphere with weak precession. *Journal of Fluid Mechanics*, 680:150–193, 2011.

[18] S. Koch, U. Harlander, C. Egbers, and R. Hollerbach. Inertial waves in a spherical shell induced by librations of the inner sphere: experimental and numerical results. *Fluid Dyn. Res.*, 45:035504, 2013.

[19] M. Le Bars, D. Cébron, and P. Le Gal. Flows driven by libration, precession, and tides. *Ann. Rev. Fluid Mech.*, 47:163–193, 2015.

[20] S. Le Dizès. Three-dimensional instability of a multipolar vortex in a rotating flow. *Phys. Fluids*, 12:2762–2774, 2000.

[21] S. Le Dizès and C. Eloy. Short-wavelength instability of a vortex in a multipolar strain field. *Phys. Fluids*, 11:500–502, 1999.

[22] J. M. Lopez and F. Marques. Instabilities and inertial waves generated in a librating cylinder. *J. Fluid Mech.*, 687:171–193, 2011.

[23] W. V. R. Malkus. Precession of the earth as the cause of geomagnetism. *Science*, 160:259–264, 1968.

[24] W. V. R. Malkus. An experimental study of global instabilities due to tidal (elliptical) distortion of a rotating elastic cylinder. *Geophys. Astrophys. Fluid Dyn.*, 48:123, 1989.

[25] C. Morize, M. Le Bars, P. Le Gal, , and A. Tilgner. Experimental determination of zonal winds driven by tides. *Phys. Rev. Lett.*, 104:214501, 2010.

[26] J. Noir, M. A. Calkins, M. Lasbleis, J. Cantwell, and J. M. Aurnou. Experimental study of libration-driven zonal flows in a straight cylinder. *Physics of the Earth and Planetary Interiors*, 182:98–1106, 2010.

[27] J. Noir, D. Cébron, M. Le Bars, A. Sauret, and J. M. Aurnou. Experimental study of libration-driven zonal flows in non-axisymmetric containers. *Physics of the Earth and Planetary Interiors*, 204-205:1–10, 2012.

[28] J. Noir, F. Hemmerlin, J. Wicht, S. Baca, and J. M. Aurnou. An experimental and numerical study of librationally driven flow in planetary cores and subsurface oceans. *Physics of the Earth and Planetary Interiors*, 173:141–152, 2009.

[29] N. Rambaux, T. Van Hoolst, and Ö. Karatekin. Librational response of Europa, Ganymede, and Callisto with an ocean for non-keplerian orbit. *A & A*, 527:A118, 2011.

[30] A. Sauret, D. Cébron, M. Le Bars, and S. Le Dizès. Fluid flows in librating cylinder. *Phys.Fluids*, 24:026603, 2012.

[31] A. Sauret, D. Cebron, C. Morize, and M. Le Bars. Experimental and numerical study of mean

zonal flows generated by librations of a rotating spherical cavity. *J. Fluid Mech.*, 662:260–268, 2010.

[32] A. Sauret, Le Bars, M., and P. Le Gal. Tide-driven shear instability in planetary liquid cores. *Geophysical Research Letters*, 41:6078–6083, 2014.

[33] A. Sauret and S. Le Dizès. Libration-induced mean flow in a spherical shell. *J. Fluid Mech*, 718:181–209, 2013.

[34] N. Schaeffer and P. Cardin. Quasigeostrophic model of the instabilities of the stewartson layer in flat and depth-varying containers. *Phys. Fluids*, 17:104111, 2005.

[35] K. Stewartson. On almost rigid rotations. *J. Fluid Mech.*, 3:17–26, 1957.

[36] K. Stewartson. On almost rigid rotations. part 2. *J. Fluid Mech.*, 26:131–144, 1966.

[37] S. T. Suess. *Some effects of gravitational tides on a rotating fluid.* PhD thesis, University of California, 1970.

[38] S. T. Suess. Viscous flow in a deformable rotating container. *J. Fluid Mech.*, 45:189–201, 1971.

[39] A. Tilgner. Zonal wind driven by inertial modes. *Phys. Rev. Lett.*, 99:194501, 2007.

[40] C.-Y. Wang. Cylindrical tank of fluid oscillating about a state of steady rotation. *J. Fluid Mech.*, 41:581–592, 1970.

[41] K. Zhang, K. H. Chan, and X. Liao. On fluid motion in librating ellipsoids with moderate equatorial eccentricity. *Journal of Fluid Mechanics*, 673:468–479, 2011.

[42] K. Zhang, P. Earnshaw, X. Liao, and F. H. Busse. On inertial waves in a rotating fluid sphere. *Journal of Fluid Mechanics*, 437:103–119, 2001.